

Neutron skin of ^{208}Pb in consistency with neutron star observations

K. Miyazaki

E-mail: miyazakiro@rio.odn.ne.jp

Abstract

The renormalized meson-nucleon couplings are applied to the relativistic optical model of p - ^{208}Pb elastic scattering at $T_{lab} = 200\text{MeV}$. We calculate the strength of the vector potential at nuclear center as varying the neutron radius of ^{208}Pb . The neutron skin thickness S_n is determined in the comparison of the calculated potential with the phenomenological one. We find a value $S_n = 0.118\text{fm}$ being consistent with the astronomical observations of massive neutron stars (NSs), the standard scenario of NS cooling and the experimental nuclear symmetry energy in terrestrial laboratory. The value is complementary to the previous result $S_n = 0.119\text{fm}$ in the analysis of elastic scattering above $T_{lab} = 500\text{MeV}$ within the relativistic impulse optical model.

Recently, there are renewed interests on the neutron skin thickness S_n of ^{208}Pb . The works [1] and [2] analyzed the nucleon-nucleus (NA) elastic scattering at low and intermediate energies within the nonrelativistic microscopic optical model, in which the nucleon-nucleon (NN) g -matrix interaction is folded by nuclear densities from the Skyrme-Hartree-Fock [1] and the RPA [2] calculations of the nucleus. They derived the values $S_n = 0.17\text{fm}$ and 0.13fm , respectively. The paper [3] analyzed the elastic scattering at high energies within the relativistic impulse optical model and obtained the value $S_n = 0.119\text{fm}$. To the contrary, Ref. [4] claimed that the elastic NA scattering is insensitive to neutron skin thickness. On the other hand, Ref. [5] derived $S_n = 0.22\text{fm}$ in the analysis of heavy-ion collisions based on an isospin- and momentum-dependent transport model, while Ref. [6] concluded $S_n \leq 0.22\text{fm}$ in the analysis of isovector giant monopole resonance within the accurately calibrated relativistic mean-field (RMF) model. Consequently, at present, the neutron radius of ^{208}Pb is not well known. The experiment of parity violating electron scattering planned at Jefferson Laboratory [7] is however likely to resolve the differences in the analyses.

This paper presents a unique method to determine the neutron skin thickness of ^{208}Pb . In the respect that we investigate the relativistic optical potential of p - ^{208}Pb elastic scattering, our work is similar to Ref. [3]. On the other hand, we are based on the RMF model of nuclear matter in Ref. [8], which has the field-dependent meson-nucleon coupling constants. The optical potential therefore includes the medium effect.

In this respect our work is similar to the $g\rho$ potential in Refs. [1] and [2]. However, in contrast to Refs. [1-3], we do not calculate the scattering cross section but the potential strength at nuclear center. In this respect we are according to Ref. [4]. Moreover, we investigate the constraints on the neutron skin from neutron star (NS) structure. Our approach is opposite to Refs. [9-11], which investigate the constraints on NS structure from the properties of finite nuclei in terrestrial laboratories. This is because [12,13] the RMF model with the field-dependent or the density-dependent meson-nucleon coupling constants is more favorable to NS matter than the nonlinear RMF model in Refs. [9-11].

In Ref. [8] we have introduced the modified meson-nucleon vertices. They are reduced to the field-dependent meson-nucleon effective coupling constants. For the proton we have

$$g_{pp\sigma(\omega)}^* = \frac{1}{2} [(1 + \lambda_0) + (1 - \lambda_0) (m_p^{*2} - v_p^2)] g_{NN\sigma(\omega)}, \quad (1)$$

$$g_{pp\delta(\rho)}^* = \frac{1}{2} [(1 + \lambda_1) + (1 - \lambda_1) (m_p^{*2} - v_p^2)] g_{NN\delta(\rho)}. \quad (2)$$

The nucleon mass is M and $V_p = v_p M$ is the vector potential. The effective mass in nuclear matter is

$$M_p^* = m_p^* M = M + S_p, \quad (3)$$

where $S_p = s_p M$ is the scalar potential. The parameter λ_0 is determined [8] so as to reproduce $m_p^* \simeq 0.6$ at saturation density. We have a value $\lambda_0 = 2/3$. The parameter λ_1 is constrained [8] so that the direct URCA process is forbidden in NSs according to the standard scenario of NS cooling. We have a condition $0 \leq \lambda_1 \leq 0.2$.

The scalar potential S_p is composed of the isoscalar and isovector parts:

$$S_p = S_{p0} + S_{p1}, \quad (4)$$

$$S_{p0} = -g_{pp\sigma}^* \langle \sigma \rangle, \quad (5)$$

$$S_{p1} = -g_{pp\delta}^* \langle \delta_3 \rangle, \quad (6)$$

where $\langle \sigma \rangle$ and $\langle \delta_3 \rangle$ are the isoscalar and isovector scalar mean-fields. From Eqs. (1) and (2), we have

$$S_{p0} = S_{p0}^{(0)} + \frac{1}{2} (1 - \lambda_0) (2s_p + s_p^2 - v_p^2) S_{p0}^{(0)}, \quad (7)$$

$$S_{p1} = S_{p1}^{(0)} + \frac{1}{2} (1 - \lambda_1) (2s_p + s_p^2 - v_p^2) S_{p1}^{(0)}, \quad (8)$$

where

$$S_{p0}^{(0)} = -g_{NN\sigma} \langle \sigma \rangle = - \left(\frac{g_{NN\sigma}}{m_\sigma} \right)^2 (\rho_{Sp} + \rho_{Sn}), \quad (9)$$

$$S_{p1}^{(0)} = -g_{NN\delta} \langle \delta_3 \rangle = - \left(\frac{g_{NN\delta}}{m_\delta} \right)^2 (\rho_{Sp} - \rho_{Sn}). \quad (10)$$

The ρ_{Sp} and ρ_{Sn} are the proton and neutron scalar densities.

The vector potential V_p is also composed of the isoscalar and isovector parts:

$$V_p = V_{p0} + V_{p1}, \quad (11)$$

$$V_{p0} = g_{pp\omega}^* \langle \omega_0 \rangle, \quad (12)$$

$$V_{p1} = g_{pp\rho}^* \langle \rho_{03} \rangle, \quad (13)$$

where $\langle \omega_0 \rangle$ and $\langle \rho_{03} \rangle$ are the isoscalar and isovector vector mean-fields. From Eqs. (1) and (2), we have

$$V_{p0} = V_{p0}^{(0)} + \frac{1}{2} (1 - \lambda_0) (2s_p + s_p^2 - v_p^2) V_{p0}^{(0)}, \quad (14)$$

$$V_{p1} = V_{p1}^{(0)} + \frac{1}{2} (1 - \lambda_1) (2s_p + s_p^2 - v_p^2) V_{p1}^{(0)}, \quad (15)$$

where

$$V_{p0}^{(0)} = g_{NN\omega} \langle \omega_0 \rangle = \left(\frac{g_{NN\omega}}{m_\omega} \right)^2 (\rho_p + \rho_n), \quad (16)$$

$$V_{p1}^{(0)} = g_{NN\rho} \langle \rho_{03} \rangle = \left(\frac{g_{NN\rho}}{m_\rho} \right)^2 (\rho_p - \rho_n). \quad (17)$$

The ρ_p and ρ_n are the proton and neutron baryon densities.

Then, we apply the above model to the relativistic optical potential of pA elastic scattering. For the purpose we identify $S_{p0}^{(0)}$, $S_{p1}^{(0)}$, $V_{p0}^{(0)}$ and $V_{p1}^{(0)}$ in Eqs. (9), (10), (16) and (17) as the $t\rho$ potentials and the second terms in Eqs. (7), (8), (14) and (15) as the medium corrections to them. This is possible because the one-meson exchange representations of NN scattering amplitudes are developed in Refs. [14-17]. We therefore assume the following replacement in Eqs. (9), (10), (16) and (17):

$$-g_{NN\sigma}^2/m_\sigma^2 \rightarrow f_{kin} F_{S0}(q=0), \quad (18)$$

$$-g_{NN\delta}^2/m_\delta^2 \rightarrow f_{kin} F_{S1}(q=0), \quad (19)$$

$$g_{NN\omega}^2/m_\omega^2 \rightarrow f_{kin} F_{V0}(q=0), \quad (20)$$

$$g_{NN\rho}^2/m_\rho^2 \rightarrow f_{kin} F_{V1}(q=0). \quad (21)$$

F_{S0} , F_{S1} , F_{V0} and F_{V1} are the isoscalar-scalar, isovector-scalar, isoscalar-vector and isovector-vector components in the Lorenz-invariant amplitude [18] of forward NN scattering. The kinematical factor f_{kin} is [15]

$$f_{kin} = \frac{4\pi p_{lab}}{M} \frac{M^2}{2E_{NN}k_{NN}}, \quad (22)$$

where p_{lab} is the momentum of the incident proton in the laboratory frame of pA scatter-

ing, and k_{NN} and E_{NN} are the momentum and the energy of nucleon in the center-of-mass frame of an elementary NN scattering in pA scattering.

The NN amplitudes in Eqs. (18)-(21) include the contribution of NN exchange scattering, which corresponds to the knockout process in pA elastic scattering. It is however well known that the exchange contribution is overestimated in the naive $t\rho$ optical potentials. This is mainly due to the pseudo-scalar pion [19], which contributes to the scalar and vector amplitudes through the Fierz exchange term. The defect can be remedied by assuming the pseudo-vector coupling in place of the pseudo-scalar one for the pion. The replacement is equivalent [15] to multiplying the pion amplitude by a factor $-Q^2/(4M^2)$. Q is the transferred 4-momentum in the NN exchange scattering.

In the present paper we concentrate on the relativistic optical potential for p- ^{208}Pb elastic scattering. Although the elastic scattering off ^{40}Ca and ^{48}Ca is analyzed in Refs. [1-3], our model based on the nuclear matter theory is appropriate only to heavy nuclei. For the calculation of $t\rho$ optical potentials, we use the NN amplitudes of Table 1 in Ref. [16] and assume the two-parameter Fermi function for the baryon densities of proton and neutron in ^{208}Pb . The diffuseness parameter 0.57fm is used so as to reproduce the experimental charge distribution in ^{208}Pb . Then, the radius parameter of proton density is fixed so as to reproduce its root-mean-square (RMS) radius $R_p \equiv \sqrt{\langle r_p^2 \rangle} = 5.45\text{fm}$ [1]. The radius parameter of neutron density is varied so that we search the RMS radius $R_n \equiv \sqrt{\langle r_n^2 \rangle}$ or the neutron skin thickness $S_n \equiv R_n - R_p$. The scalar densities of proton and neutron in ^{208}Pb are calculated according to Eq. (3.4) in Ref. [15] but with the effective nucleon mass $M^* = 0.6M$ in the saturated nuclear matter.

Once the $t\rho$ potentials $S_{p0}^{(0)}$, $S_{p1}^{(0)}$, $V_{p0}^{(0)}$ and $V_{p1}^{(0)}$ are given, we can evaluate the proper optical potentials from Eqs. (7), (8), (14) and (15). They are determined self-consistently because the second terms in the equations contain them. In this paper we consider the strength of the potential at the center of ^{208}Pb . As the neutron radius or the neutron skin thickness is larger, the strength becomes weaker. If the strength is well known, the neutron skin thickness can be found. Fortunately, we have the relativistic optical model potential [20], which is phenomenologically determined so as to reproduce pA elastic scattering data. It is highly reliable because it is able to reproduce the data over the wide range of the energy and the nucleus.

There still remains a problem to specify the proton incident energy T_{lab} at which the optical potential is evaluated. At higher energy than $T_{lab} = 500\text{MeV}$ the impulse approximation [3] is relatively good. Because the medium effect is a key ingredient in studying the correlation between the dilute neutron skin and the dense NS matter, we should study at much lower energy. On the other hand, at lower energy than $T_{lab} = 100\text{MeV}$ we cannot expect that our relativistic optical model based on the RMF approximation works well. In the following numerical analyses we therefore assume $T_{lab} = 200\text{MeV}$, which is the highest energy in the nonrelativistic $g\rho$ optical model of Ref. [1] but is the lowest energy in the Lorenz invariant NN amplitude of Ref. [16].

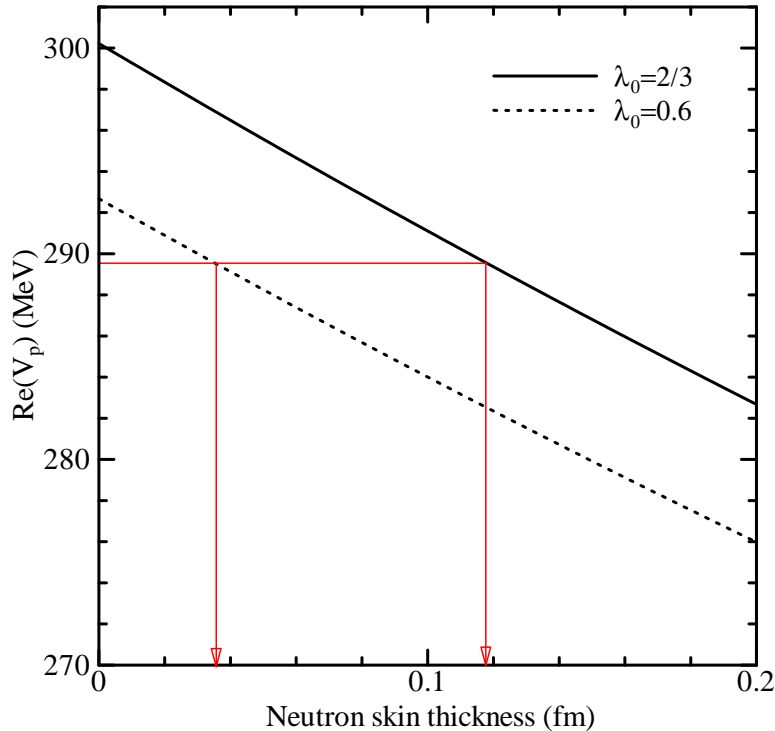


Figure 1: The central strength of the real vector potential for p- ^{208}Pb optical model at $T_{lab} = 200\text{MeV}$ as a function of the neutron skin thickness. The black solid line is the calculation using $\lambda_0 = 2/3$ and $\lambda_1 = 0$ in Eqs. (1) and (2), while the dotted line is the result using $\lambda_0 = 0.6$ and $\lambda_1 = 0$. The horizontal red line is the strength of the phenomenological optical potential of Table II in Ref. [20].

Figure 1 shows the strength of the real vector potential at the center of ^{208}Pb as a function of the neutron skin thickness. The scalar potential is not useful for our purpose because it does not straightforwardly reflect the baryon density distribution in a nucleus. The imaginary part of the potential cannot be calculated precisely in our model based on the nuclear matter theory. Therefore, we do not analyze the scattering data in contrast to Refs. [1-3]. The strength decreases linearly as the neutron skin becomes thicker. The black solid line is the result using $\lambda_0 = 2/3$ and $\lambda_1 = 0$ in Eqs. (1) and (2). The value of λ_0 is determined [8] so as to reproduce the effective nucleon mass $M^* = 0.6M$ in the saturated nuclear matter. The value of λ_1 is appropriate [8] to reproduce the experimental density dependence [21-23] of the nuclear symmetry energy at sub-saturation densities. The horizontal red line indicates the phenomenological optical potential of Table II in Ref. [20]. The intersection of the two lines determines the neutron skin thickness of ^{208}Pb . We have a value $S_n = 0.118\text{fm}$, which agrees well with $S_n = 0.119\text{fm}$ obtained from the most systematic analysis in Ref. [3]. If we use the NN amplitude of Table 2 in Ref. [16], the vector potential is much stronger than the black line. If we use the phenomenological optical potential of Table III in Ref. [20], the red horizontal line falls down largely. They are however inappropriate because the calculated strength cannot

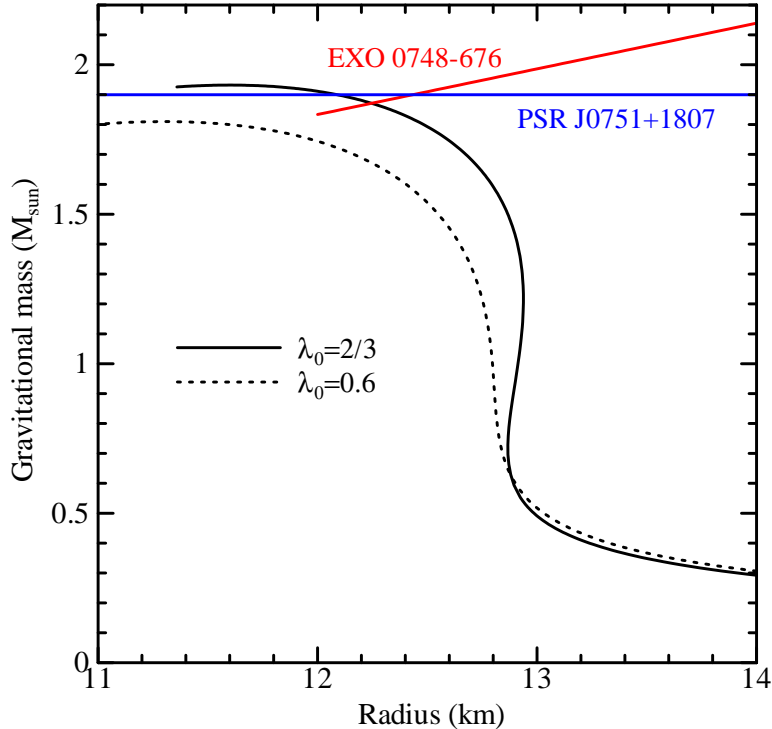


Figure 2: The mass-radius relation of NS. The black solid and dotted curves are calculated using the EOSs of NS matter in the RMF model of Ref. [8] with $\lambda_0 = 2/3$ and $\lambda_0 = 0.6$, respectively. The red line is the mass-radius relation of EXO 0748-676 derived in Ref. [25]. The horizontal blue line indicates the lower limit $M_G = 1.9M_\odot$ [29] of the observed massive NS in PSR J0751+1807.

agree with the phenomenological one in the reasonable range of neutron skin thickness.

As λ_0 is larger in Eq. (1), the equation-of-state (EOS) of nuclear matter is stiffer. The incompressibility $K = 320\text{MeV}$ [8] for $\lambda_0 = 2/3$ is close to the upper limit of the experimental value $K = 300 \pm 25\text{MeV}$ in Ref. [24]. Therefore, the larger value than $2/3$ is not considered. To the contrary, a somewhat smaller value $\lambda_0 = 0.6$ is possible because the incompressibility is $K = 292\text{MeV}$. The black dotted line in Fig. 1 is the calculation using the value. The reason that the dotted line is lower than the solid line is understood as follows. Taking into account $|s_p^2 - v_p^2| \ll |2s_p|$, Eq. (14) is approximated by

$$V_{p0} \approx [1 + (1 - \lambda_0) s_p] V_{p0}^{(0)}. \quad (23)$$

Because the scalar potential is negative, V_{p0} becomes stronger as λ_0 is larger. Furthermore, because the isoscalar potential V_{p0} is dominant over the isovector one V_{p1} in Eq. (11), the total vector potential V_p also becomes stronger as λ_0 is larger. So as to reproduce the phenomenological potential strength we have a value $S_n = 0.035\text{fm}$ for $\lambda_0 = 0.6$. Comparing the value with $S_n = 0.118\text{fm}$ for $\lambda_0 = 2/3$ it is seen that the neutron skin thickness strongly depends on the effective isoscalar meson-nucleon coupling constants.

Is the rather thin neutron skin $S_n = 0.035\text{fm}$ physically allowed? In order to answer

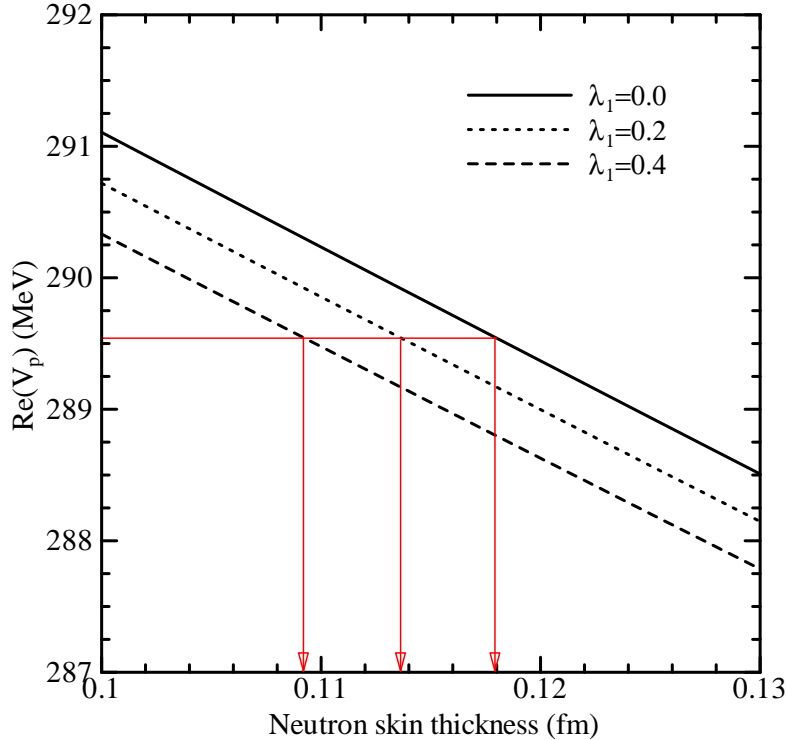


Figure 3: The same as Fig. 1 but for $\lambda_1 = 0.0$, $\lambda_1 = 0.2$ and $\lambda_1 = 0.4$ with $\lambda_0 = 2/3$.

the question we show in Fig. 2 that the observation of NS is useful to constrain the neutron skin thickness of ^{208}Pb . The black solid and dotted curves are the mass-radius relations of NS calculated using the EOSs of $\lambda_0 = 2/3$ and $\lambda_0 = 0.6$ in Eq. (1), respectively. The detailed numerical method is the same as Fig. 2 in Ref. [8]. The red line is the observed mass-radius relation of EXO 0748-676 in Ref. [25]. If we assume [26-28] that it is a good criterion for a reasonable EOS of NS matter, the dotted curve is ruled out. Consequently, the thin neutron skin $S_n = 0.035\text{fm}$ is not realized. The conclusion is also supported by the recently observed massive NS of $M_G = 2.1 \pm 0.2M_\odot$ [29] in PSR J0751+1807. Inversely, the exclusion of the thin neutron skin [1-6] supports the observations of the massive NSs.

Next, we investigate the effect of the isovector meson-nucleon couplings on the neutron skin. The solid, dotted and dashed lines in Fig. 3 show the strengths of the real vector potential for $\lambda_1 = 0.0$, 0.2 and 0.4 , respectively. All the calculations assume $\lambda_0 = 2/3$. As Eq. (23), Eq. (15) is also approximated by

$$V_{p1} \approx [1 + (1 - \lambda_1) s_p] V_{p1}^{(0)}. \quad (24)$$

Because ρ_n is larger than ρ_p in ^{208}Pb , $V_{p1}^{(0)}$ of Eq. (17) is negative. Therefore, as λ_1 is larger, V_{p1} becomes deeper and so the total vector potential V_p becomes weaker. So as to reproduce the phenomenological potential strength depicted by horizontal red line we have $S_n = 0.1137\text{fm}$ and 0.1091fm for $\lambda_1 = 0.2$ and 0.4 , respectively. The sensitivity of

the neutron skin to λ_1 is much weaker than the sensitivity to λ_0 . It is shown in Ref. [8] that according to the standard scenario of NS cooling in which the direct URCA process is forbidden, the value $\lambda_1 \geq 0.4$ is not allowed. Consequently, the neutron skin thickness should be larger than 0.11fm. The condition is much severer than the allowed range of S_n in Ref. [3]. This also indicates that the NS structure constrains the neutron skin.

Finally, it is worthwhile to compare our result with Ref. [11], which is based on the nonlinear RMF model referred to "FSUGold". The model predicts a rather thick neutron skin $S_n = 0.21\text{fm}$ of ^{208}Pb . In its calculation of NS structure, the mass and radius cannot reproduce EXO 0748-676, and the direct URCA cooling is allowed. The results are evidently contrasted to ours and suggest the essential difference between the RMF models with and without the field-dependent effective meson-nucleon coupling constants. Moreover, the latter model cannot be applied to the optical potential of pA elastic scattering at intermediate energy.

We apply the RMF model of nuclear matter developed in Ref. [8] to the relativistic optical model of p- ^{208}Pb elastic scattering at $T_{lab} = 200\text{MeV}$. The optical potential includes the medium correction to the $t\rho$ potential through the renormalized meson-nucleon coupling constants. We calculate the strength of the real vector potential at nuclear center as varying the neutron radius of ^{208}Pb . The neutron skin thickness is determined in the comparison of the calculated strength with the phenomenological potential fitted to the elastic scattering data. It is found that the observations of NS are useful to constrain the neutron radius. The observed mass-radius relation of EXO 0748-676 and the massive NS in PSR J0751+1807 exclude the rather thin neutron skin through the isoscalar coupling constants. The standard scenario of NS cooling limits the lowest skin thickness more severely through the isovector coupling constants. Taking into account the density dependence of the nuclear symmetry energy in the recent works [21-23], we conclude that the neutron skin thickness $S_n = 0.118\text{fm}$ is the most reasonable. The value well agrees with the result $S_n = 0.119\text{fm}$ in the analysis of elastic scattering above $T_{lab} = 500\text{MeV}$ within the relativistic impulse optical model. Because our result is based on the optical potential at $T_{lab} = 200\text{MeV}$ corrected by medium against the impulse one, both the results are complementary to each other.

References

- [1] S. Karataglidis, K. Amos, B.A. Brown and P.K. Deb, Phys. Rev. C **65** (2002) 044306.
- [2] M. Dupuis, S. Karataglidis, E. Bauge, J.-P. Delaroche and D. Gogny, arXiv:nucl-th/0506077.
- [3] B.C. Clark, L.J. Kerr and S. Hama, Phys. Rev. C **67** (2003) 054605 [arXiv:nucl-th/0209052].
- [4] J. Piekarewicz and S.P. Weppner, Nucl. Phys A **778** (2006) 10 [arXiv:nucl-th/0509019].
- [5] L.-W. Chen, C.M. Ko and B.-A. Li, Phys. Rev. C **72** (2005) 064309 [arXiv:nucl-th/0509009].
- [6] J. Piekarewicz, Phys. Rev. C **69** (2004) 041301 [arXiv:nucl-th/0312020].
- [7] R. Michaels *et al.*, "A CLEAN MEASUREMENT OF THE NEUTRON SKIN OF ^{208}Pb THROUGH PARITY VIOLATING ELECTRON SCATTERING" (2005) on <http://hallaweb.jlab.org/parity/prex>
- [8] K. Miyazaki, Mathematical Physics Preprint Archive (mp_arc) 06-336.
- [9] C.J. Horowitz and J. Piekarewicz, Phys. Rev. Lett. **86** (2001) 5647.
- [10] C.J. Horowitz and J. Piekarewicz, Phys. Rev. C **66** (2002) 055803 [arXiv:nucl-th/0209052].
- [11] B.G. Todd-Rutel and J. Piekarewicz, Phys. Rev. Lett. **95** (2005) 122501 [arXiv:nucl-th/0504034].
- [12] T. Klähn *et al.*, arXiv:nucl-th/0602038.
- [13] K. Miyazaki, Mathematical Physics Preprint Archive (mp_arc) 06-103.
- [14] C.J. Horowicz, Phys. Rev. C **31** (1985) 1340.
- [15] D.P. Murdock and C.J. Horowicz, Phys. Rev. C **35** (1987) 1442.
- [16] O.V. Maxwell, Nucl. Phys. A **600** (1996) 509.
- [17] O.V. Maxwell, Nucl. Phys. A **638** (1998) 747.
- [18] J.A. McNeil, J.R. Shepard and S.J. Wallace, Phys. Rev. Lett. **50** (1983) 1439.
- [19] J.A. Tjon and S.J. Wallace, Phys. Rev. C **32** (1985) 267.

- [20] S. Hama, B.C. Clark, E.D. Cooper, H.S. Sherif and R.L. Mercer, Phys. Rev. C **41** (1990) 2737.
- [21] B-A. Li and L-W. Chen, Phys. Rev. C **72** (2005) 064611 [arXiv:nucl-th/0508024].
- [22] Z-H. Li, L-W. Chen, C.M. Ko, B-A. Li and H-R. Ma, Phys. Rev. C **74** (2006) 044613 [arXiv:nucl-th/0606063].
- [23] D.V. Shetty, S.J. Yennello and G.A. Souliotis, arXiv:nucl-ex/0610019.
- [24] M.M. Sharma, W.T.A. Borghols, S. Brandenburg, S. Corna, A. van der Woude and M.N. Harakeh, Phys. Rev. C **38** (1988) 2562.
- [25] F. Özel, Nature **441** (2006) 1115 [arXiv:astro-ph/0605106].
- [26] M. Alford, D. Blaschke, A. Drago, T. Klähn, G. Pagliara and J. Schaffner-Bielich, arXiv:astro-ph/0606524.
- [27] P. Jaikumar, S. Reddy and A.W. Steiner, arXiv:astro-ph/0608345.
- [28] T. Klähn *et al.*, arXiv:nucl-th/0609067.
- [29] D.J. Nice *et al.*, Astrophys. J. **634** (2005) 1242 [arXiv:astro-ph/0508050].